

# Unlocking the Forgery Detection Potential of Vanilla MLLMs: A Novel Training-Free Pipeline

Rui Zuo  
Zhejiang University  
22431088@zju.edu.cn

Qinyue Tong  
Zhejiang University  
qinyuetong@zju.edu.cn

Zhe-Ming Lu  
Zhejiang University  
zheminglu@zju.edu.cn

Ziqian Lu  
Zhejiang Sci-Tech University  
ziqianlu@zstu.edu.cn

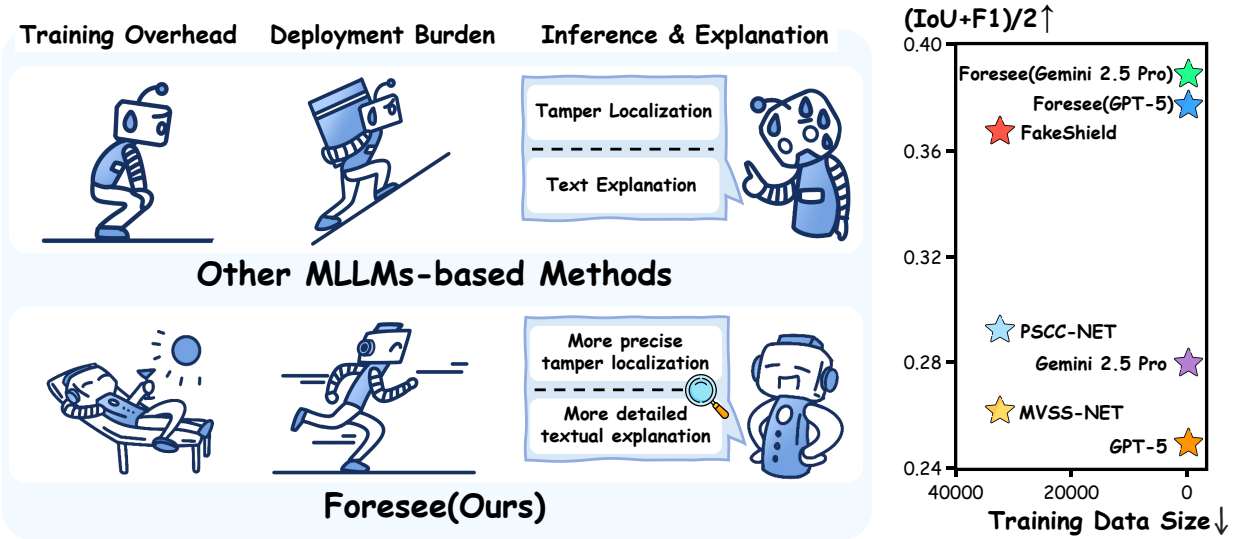


Figure 1. Comparison of our Foresee pipeline with other state-of-the-art MLLM-based methods and vanilla MLLMs in terms of training overhead, deployment burden, and inference performance. Foresee surpasses existing MLLM-based tamper detection methods by operating without any training, requiring fewer computational and inference resources, providing more precise localization, and delivering richer textual explanations. Notably, vanilla MLLMs achieve a significant improvement in localization performance under our pipeline.

## Abstract

With the rapid advancement of artificial intelligence-generated content (AIGC) technologies, including multi-modal large language models (MLLMs) and diffusion models, image generation and manipulation have become remarkably effortless. Existing image forgery detection and localization (IFDL) methods often struggle to generalize across diverse datasets and offer limited interpretability. Nowadays, MLLMs demonstrate strong generalization potential across diverse vision-language tasks, and some studies introduce this capability to IFDL via large-scale training. However, such approaches cost considerable computational resources, while failing to reveal the inherent generalization potential of vanilla MLLMs to address this

problem. Inspired by this observation, we propose **Foresee**, a **training-free MLLM-based pipeline** tailored for image forgery analysis. It eliminates the need for additional training and enables a lightweight inference process, while surpassing existing MLLM-based methods in both tamper localization accuracy and the richness of textual explanations. Foresee employs a **type-prior-driven strategy** and utilizes a **Flexible Feature Detector (FFD)** module to specifically handle copy-move manipulations, thereby effectively unleashing the potential of vanilla MLLMs in the forensic domain. Extensive experiments demonstrate that our approach simultaneously achieves superior localization accuracy and provides more comprehensive textual explanations. Moreover, Foresee exhibits stronger generalization capability, outperforming existing IFDL methods across

various tampering types, including copy-move, splicing, removal, local enhancement, deepfake, and AIGC-based editing. The code will be released in the final version.

## 1. Introduction

With the rapid advancement of artificial intelligence-generated content (AIGC) technologies, including multimodal large language models (MLLMs) [4, 19, 28, 43, 45] and diffusion models [40, 41], the generation and manipulation of images have become remarkably effortless. In practical scenarios, users simply provide an original image along with their specific requirements to multimodal generative AI models, such as Qwen-VL [48] and Sora [37], which can then perform editing manipulations that previously would have required substantial manual effort. This paradigm enables the creation of highly realistic or entirely fictitious images with minimal exertion. While such capabilities greatly benefit creative industries, they also introduce significant risks—facilitating the spread of misinformation, enabling identity fraud, and compromising personal privacy. Consequently, the development of robust image forgery detection and localization (IFDL) strategies has emerged as an urgent challenge in ensuring social trust and security.

IFDL has advanced rapidly [54, 55]; however, mainstream methods [11, 17, 22, 30, 33] typically demonstrate strong performance only on specific datasets, limiting their generalizability. Recent methods [55, 56] attempt to leverage diffusion models for more precise identification of manipulation boundaries to alleviate this limitation. Despite their advancements, these methods still exhibit considerable room for improvement in generalization. Nowadays, MLLMs demonstrate impressive capabilities across a wide range of vision-language tasks, exhibiting substantial generalization potential [28, 38, 45, 57]. Therefore, FakeShield [54] introduces the generalization capability of MLLMs into the image forgery detection domain through large-scale training. Despite the success, it costs considerable training and computational resources. Motivated by this observation, we raise a fundamental question: “Do vanilla MLLMs inherently possess the generalization potential to address this problem, which has simply yet to be uncovered?”

Inspired by this, we first attempt to directly employ vanilla MLLMs [3, 9, 15, 38] to address the image manipulation problem; however, the results are unsatisfactory, as shown in Figure 2, their responses fall short of expectations—these models tend to overlook fine-grained tampering clues and often provide overly general or semantically plausible explanations instead of identifying the actual manipulations. To overcome these limitations, we propose **Foresee**, a training-free MLLM-based pipeline tailored for

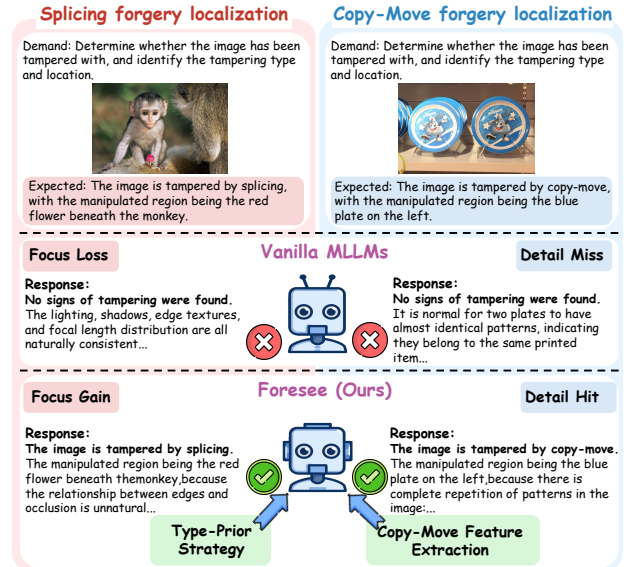


Figure 2. Qualitative comparison between vanilla MLLMs and our Foresee pipeline on *splicing* and *copy-move* cases in the IFDL task, illustrating Foresee’s improved localization accuracy.

interpretable image forgery analysis. As illustrated in Figure 1, Foresee eliminates the need for additional training and enables a lightweight inference process, while surpassing existing MLLM-based methods in both tamper localization accuracy and the richness of textual explanations. The right side of Figure 1 further demonstrates that the proposed pipeline achieves superior localization performance with significantly less training data compared to state-of-the-art methods, highlighting its strong generalization capability across diverse data distributions. Figure 2 intuitively illustrates performance that demonstrates the potential of vanilla MLLMs unleashed by Foresee in image forgery detection. Our pipeline augments vanilla MLLMs with a type-prior-driven reasoning process and supplies copy-move-specific feature extraction hints, enabling accurate identification of various manipulation types (e.g., *splicing*, *copy-move*) and providing more insightful textual explanations.

Specifically, Foresee leverages a type-prior-driven strategy to first determine the manipulation type of the input image, thereby guiding the MLLM to better focus on tampering traces relevant to each category. This step is followed by MLLM-guided inference and segmentation to jointly produce explanatory texts and localization masks. In addition, Foresee integrates a dedicated *copy-move* detection module to compensate for the limited capability of vanilla MLLMs in recognizing self-consistent forgeries. Together, these components constitute a training-free, generalizable, and interpretable forensic pipeline for IFDL. Our main contributions are summarized as follows:

- We present the first attempt to explore the direct application of vanilla MLLMs to the image forgery detection

and localization (IFDL) task and propose a novel training-free pipeline named **Foresee**. Foresee not only alleviates generalization and interpretability limitations in existing IFDL approaches, but also substantially reduces dependence on large-scale training data and computationally resources that constrain interpretable models.

- We introduce a **Flexible Feature Detector (FFD)** module, which incorporates interchangeable training-free approaches for processing *copy-move* manipulated images.
- Our work fills the gap in image forgery localization for training-free methods. Extensive experiments demonstrate that our approach achieves superior localization accuracy, provides more comprehensive textual explanations, and exhibits stronger generalization capability, outperforming existing IFDL methods across diverse tampering types including *copy-move*, *splicing*, *removal*, *local enhancement*, *deepfake*, and *AIGC-based editing*.

## 2. Related Work

### 2.1. Image Forgery Detection and Localization

Traditional forgery detection methods [2, 8, 14, 20, 24, 27, 42, 52, 58] have primarily focused on identifying a single type of manipulation and generally lack robust localization capabilities. In recent years, mainstream approaches [11, 17, 18, 22, 30, 33, 51, 53] for image forgery detection and localization have increasingly emphasized model generalization, aiming to detect a wide range of manipulation types. Most of these approaches are based on convolutional neural networks or transformer architectures, leveraging pixel-level or learned feature representations to identify forgery traces. Although these methods achieve considerable success, they still often fall short in terms of generalization to diverse manipulation types. Recently, more novel methods [47, 55] employing diffusion models have emerged, which help to mitigate the generalization limitations of previous approaches. Concurrently, a fine-tuned large language model [54] for IFDL tasks not only improve generalization, but also introduce a new paradigm of textual interpretation for the task. However, these state-of-the-art methods typically require substantial computational resources, which presents additional challenges for practical deployment of image forgery detection and localization. Fortunately, a recent training-free method [56], utilizing diffusion and custom-designed modules aims to alleviate these constraints. Nevertheless, its localization performance still lags behind that of models trained specifically for this task. These limitations highlight the need for more efficient, generalizable, and interpretable approaches to image forgery detection and localization, motivating the development of our proposed method.

### 2.2. MLLMs on Detection Tasks

The application of Multimodal Large Language Models (MLLMs) to detection tasks has recently become an area of active research [6, 28, 45]. A prevalent approach involves fine-tuning MLLMs on high-quality image-text instruction datasets centered around detection scenarios. For instance, several recent methods [26, 28, 57] construct detailed question-answer pairs that cover diverse detection cases. However, this process demands significant manual annotation and considerable computational resources, yet still struggles to generalize to unseen objects. Additionally, as most cutting-edge MLLMs remain closed-source [3, 15, 38], further instruction tuning is often impractical. In this work, we explore the inherent zero-shot detection capability of vanilla MLLMs to generalize across diverse types of image manipulations. Accordingly, we propose a novel training-free pipeline based on MLLMs, which decomposes the reasoning process through a Chain-of-Thought paradigm and leverages conventional forgery detection techniques as contextual cues for vanilla MLLMs. This strategy serves to fully unlock the potential of MLLMs in the domain of image forgery detection and localization.

## 3. Methodology

While state-of-the-art MLLMs, such as GPT-5 [38] and Gemini 2.5 Pro [15], exhibit impressive visual reasoning and recognition capabilities, their potential for identifying manipulated images is still unleashed. To fully unlock the capabilities of MLLMs in uncovering image forgeries, we introduce a training-free, MLLM-based pipeline named Foresee that decomposes the tampering detection process through the chain-of-thought [21, 49] reasoning paradigm, enabling MLLMs to adapt more smoothly to IFDL tasks. The overview pipeline of the proposed Foresee is illustrated in Figure 3, which comprises: forgery-type prediction and task-specific prompt selection (Section 3.1), followed by MLLM-guided inference and segmentation to produce explanations and masks (Section 3.2). In addition, we introduce a dedicated *copy-move* detection module to compensate for the limited abilities of vanilla MLLMs to recognize self-consistent forgeries (Section 3.3). The pseudocode outlining the complete pipeline is provided in Algorithm 1.

### 3.1. Forgery-Type Prediction and Prompt Selection

When directly applied to manipulated images, general-purpose MLLMs often struggle to maintain stable and coherent reasoning, primarily due to their tendency to conflate different types of tampering. Therefore, we adopt a type-prior-driven strategy that guides the MLLM to perform tampering analysis in a step-by-step manner. Specifically, we first instruct the MLLM to identify the tampering type using a meticulously designed prompt that embeds de-

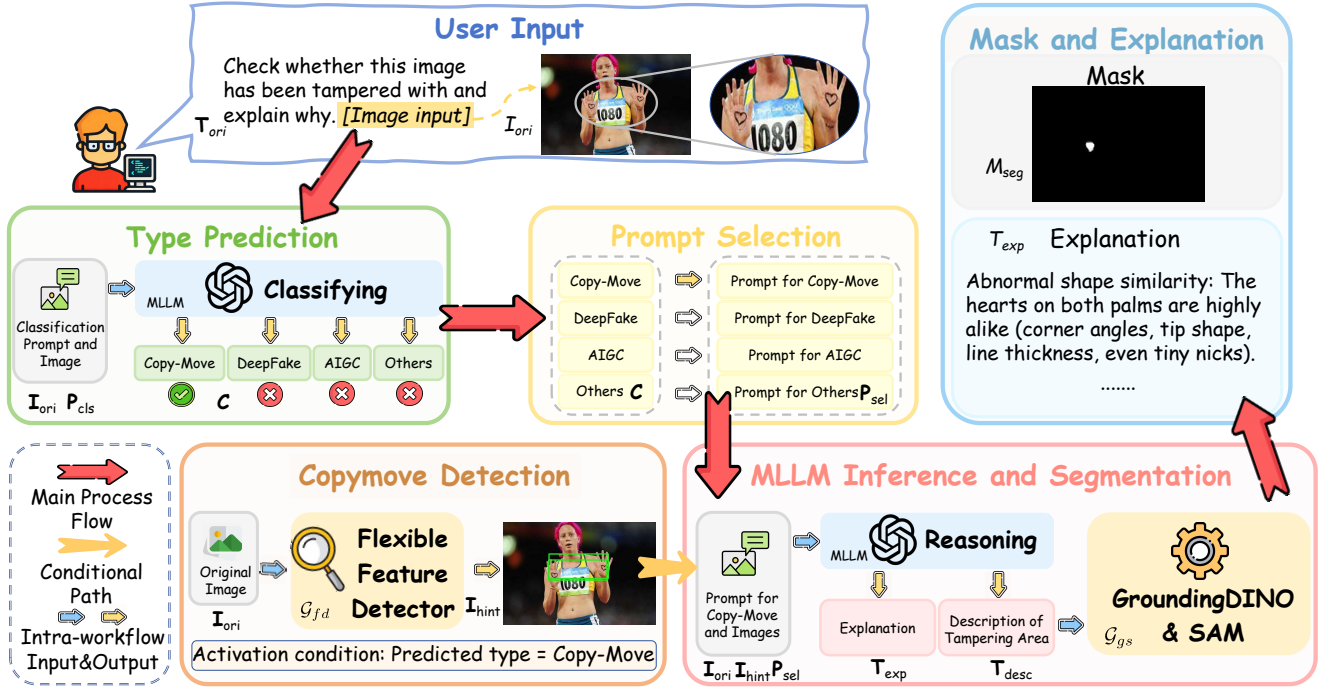


Figure 3. Overview of the proposed Foresee pipeline. The input image  $\mathbf{I}_{ori}$  and classification prompt  $\mathbf{P}_{cls}$  are processed by MLLM to predict the classification label  $\mathbf{C}$ . If  $\mathbf{C}$  indicates copy-move, the Flexible Feature Detector  $\mathcal{G}_{fd}$  generates a hint image  $\mathbf{I}_{hint}$ . Then,  $\mathbf{I}_{ori}$ ,  $\mathbf{I}_{hint}$  (if available), and a task-specific prompt  $\mathbf{P}_{sel}$  are fed into MLLM to produce a textual explanation  $\mathbf{T}_{exp}$  and a concise description  $\mathbf{T}_{desc}$  of the tampered region. Finally,  $\mathbf{T}_{desc}$  guides the Grounded Segmentation Module  $\mathcal{G}_{gs}$  to generate the tampering mask  $\mathbf{M}_{seg}$ .

scriptive features of different tampering categories, thereby facilitating more accurate classification. To facilitate this process, Foresee adopts a four-way taxonomy inspired by prior work [33, 35], covering *copy-move*, *deepfake*, *AIGC*, and *others*. These types correspond to distinct forensic evidence patterns: *copy-move* emphasizes intra-image duplication and abnormally consistent textures [8, 13, 14]; *deepfake* focuses on facial appearance edits [44, 46]; *AIGC-based* methods target inconsistencies between local regions and the whole image in illumination noise statistics [5, 31]; the *others* category covers splicing, removal, and local enhancement, which typically manifest as seam artifacts, boundary halos, and semantic inconsistencies [7, 10, 25].

As shown in Figure 3, the input image  $\mathbf{I}_{ori}$ , together with the classification prompt  $\mathbf{P}_{cls}$ , is provided to the MLLM for joint processing, which outputs an image classification label  $\mathbf{C}$ . Notably, during this process, a tentative tampering type is assigned to every input image, regardless of whether manipulation is present; the following reasoning phase will determine whether manipulation exists. Subsequently, a corresponding type-aligned prompt  $\mathbf{P}_{sel}$  is selected to steer the MLLM toward the most discriminative tampering traces and spatial cues associated with that category. The process can be formulated as:

$$\mathbf{C} = \text{MLLM}(\mathbf{I}_{ori}, \mathbf{P}_{cls}), \quad (1)$$

$$\mathbf{P}_{sel} = \mathbf{P}_{sel}^{(\mathbf{C})}. \quad (2)$$

This task-prior design incorporates the chain-of-thought paradigm, effectively alleviating the reasoning burden of the MLLM in subsequent inference stages.

### 3.2. MLLM Inference and Segmentation

Building upon the prompt selection and task-prior strategy described previously, this stage leverages the MLLMs to perform comprehensive tampering analysis, and utilizes its outputs to activate GroundingDINO [29] and SAM2 [39] to accomplish mask segmentation. Specifically, the pipeline utilizes the input image  $\mathbf{I}_{ori}$ , a hint image cue tailored for *copy-move* tampering  $\mathbf{I}_{hint}$  (obtained by the Flexible Feature Detector module  $\mathcal{G}_{fd}$ ), and the category-specific prompt  $\mathbf{P}_{sel}$  to steer the MLLM’s reasoning process. The model generates a comprehensive, multi-faceted textual explanation  $\mathbf{T}_{exp}$  and a concise yet effective description of the suspected tampering area  $\mathbf{T}_{desc}$  (e.g., “a heart-shaped doodle on the athlete’s left hand”). The description  $\mathbf{T}_{desc}$  is subsequently utilized by **Grounded Segmentation Module**  $\mathcal{G}_{gs}$ , including GroundingDINO and SAM, where GroundingDINO leverages its strong text–region alignment capability to precisely localize the tampered area described by  $\mathbf{T}_{desc}$ , providing accurate spatial coordinates for subsequent segmentation. The grounded regions are subsequently utilized by SAM2, which produces precise segmen-

Table 1. Detection performance comparison of various IFDL methods and vanilla MLLMs across multiple editing, deepfake, and AIGC-editing datasets, covering both traditional and generative manipulations types. The best and second-best results are highlighted in bold and underline, respectively. Explanation availability is indicated by  $\checkmark/\times$ .  $\dagger$ : Partially self-tested.  $\ddagger$ : Fully self-tested.

Method	Explanation	Editing					DeepFake	AIGC-Editing	Average
		CASIA1.0+	Columbia	Coverage	NIST16	IMD2020	FaceApp	OpenForensics	
image-level AUC									
<i>trained methods</i>									
HiFi-Net $\dagger$ [17]	$\times$	46.0	68.0	34.0	58.8	62.0	56.0	28.0	50.4
PSCC-Net $\dagger$ [30]	$\times$	<u>90.0</u>	78.0	84.0	61.3	67.0	48.0	39.5	66.8
MVSS-Net $\dagger$ [11]	$\times$	62.0	94.0	65.0	<u>72.3</u>	75.0	<u>84.0</u>	45.5	71.2
FakeShield $\dagger$ [54]	$\checkmark$	<b>95.0</b>	98.0	<b>97.0</b>	<b>74.8</b>	<b>83.0</b>	<b>93.0</b>	37.5	<b>82.5</b>
<i>vanilla MLLMs</i>									
GPT-5 [38]	$\checkmark$	70.7	97.5	71.0	66.3	77.3	61.0	48.5	70.3
Gemini 2.5 Pro [15]	$\checkmark$	72.4	<u>98.5</u>	73.5	64.2	73.2	67.0	53.0	71.7
<i>training-free methods</i>									
Noise $\ddagger$ [7, 14, 32]	$\times$	28.1	46.3	69.5	17.3	21.9	6.0	3.5	27.5
Block $\ddagger$ [2, 14]	$\times$	25.8	40.6	76.0	12.4	23.7	2.5	5.0	26.6
Point $\ddagger$ [8, 14, 52]	$\times$	34.5	25.6	81.0	21.6	31.0	8.0	4.0	29.4
Foresee(GPT-5)	$\checkmark$	83.2	97.5	85.5	69.0	<u>78.6</u>	<u>84.0</u>	<u>50.0</u>	78.3
Foresee(Gemini 2.5 Pro)	$\checkmark$	86.6	<b>99.0</b>	<u>87.5</u>	68.3	74.1	<b>93.0</b>	<b>57.5</b>	80.9

tation masks  $\mathbf{M}_{seg}$ , thereby enhancing the accuracy of tampering localization. This process can be formulated as:

$$\mathbf{I}_{hint} = \mathcal{G}_{fd}(\mathbf{I}_{ori}), \quad (3)$$

$$\mathbf{T}_{exp}, \mathbf{T}_{desc} = \text{MLLM}(\mathbf{I}_{ori}, \mathbf{I}_{hint}, \mathbf{P}_{sel}), \quad (4)$$

$$\mathbf{M}_{seg} = \mathcal{G}_{gs}(\mathbf{T}_{desc}). \quad (5)$$

---

#### Algorithm 1 Overall Tampering Detection Pipeline

---

- 1: **Input:** User input image  $\mathbf{I}_{ori}$ , classification prompt  $\mathbf{P}_{cls}$
  - 2: **Output:** Tampering mask  $\mathbf{M}_{seg}$ , explanation  $\mathbf{T}_{exp}$
  - 3: Predict tampering type  $\mathbf{C} = \text{MLLM}(\mathbf{I}_{ori}, \mathbf{P}_{cls})$
  - 4: Select category-specific prompt  $\mathbf{P}_{sel}$  according to  $\mathbf{C}$ ,  
 $\mathbf{P}_{sel} = \mathbf{P}_{sel}^{(\mathbf{C})}$
  - 5: **if**  $\mathbf{C} == \text{Copy-Move}$  **then**
  - 6:     Generate hint image  $\mathbf{I}_{hint} = \mathcal{G}_{fd}(\mathbf{I}_{ori})$
  - 7: **else**
  - 8:      $\mathbf{I}_{hint} \leftarrow \text{None}$
  - 9: **end if**
  - 10: Input  $\mathbf{I}_{ori}$ ,  $\mathbf{I}_{hint}$  (if available), and  $\mathbf{P}_{sel}$  to MLLM
  - 11: Obtain explanation  $\mathbf{T}_{exp}$  and description of tampering area  $\mathbf{T}_{desc}$ ,  
 $\mathbf{T}_{exp}, \mathbf{T}_{desc} = \text{MLLM}(\mathbf{I}_{ori}, \mathbf{I}_{hint}, \mathbf{P}_{sel})$
  - 12: GroundingDINO localizes region based on  $\mathbf{T}_{desc}$
  - 13: SAM refines the region to generate final mask  $\mathbf{M}_{seg}$ ,  
 $\mathbf{M}_{seg} = \mathcal{G}_{gs}(\mathbf{T}_{desc})$ .
  - 14: Return  $\mathbf{M}_{seg}$  and  $\mathbf{T}_{exp}$  as final results
- 

In Formula 3,  $\mathbf{I}_{hint}$  is produced by the Flexible Feature Detector module. This module is triggered only when the inferred tampering type is *copy-move*, since we observe that MLLMs tend to struggle with *copy-move* forgeries—primarily due to the subtlety of duplicated textures

and the lack of well-defined tampering boundaries. We describe the design and implementation of this module in detail below.

### 3.3. Flexible Feature Detector Module

To address the unique challenges posed by *copy-move* tampering, where duplicated textures are often subtle and tampering boundaries are indistinct, we propose a **Flexible Feature Detector** module (FFD). This module is selectively activated when the image’s predicted tampering type is *copy-move*. It incorporates a set of interchangeable, training-free approaches, such as noise-based [7, 14, 32], block-based [2, 14], and keypoint-based methods [8, 14, 52], to extract and highlight potential regions of repeated textures within the original image  $\mathbf{I}_{ori}$ . They possess unique advantages over trained methods when dealing with *copy-move* tampered images, such as being straightforward to implement, highly reproducible, and enabling fast inference, rendering them well-suited as hint image generators for the MLLM. Moreover, block-based and keypoint-based methods are specifically tailored for *copy-move* tampering, effectively compensating for the inherent limitations of the MLLM in detecting duplicated textures. By leveraging these specialized feature extraction strategies, our pipeline enables the MLLM to discriminate self-consistent forgery patterns more effectively, thereby enhancing the performance in *copy-move* manipulation localization. The pseudocode of our proposed Foresee is presented in Algorithm 1.

## 4. Experiments

### 4.1. Experimental Setup

**Dataset:** Considering the availability and generality, we select several challenging benchmark datasets to evaluate

Table 2. Localization performance comparison of various IFDL methods and vanilla MLLMs across multiple editing, deepfake, and AIGC-editing datasets, covering both traditional and generative manipulations types. The best and second-best results are highlighted in bold and underline, respectively. Explanation availability is indicated by  $\checkmark/\times$ .  $\dagger$ : Partially self-tested.  $\ddagger$ : Fully self-tested.

Method	Explanation	Editing					DeepFake	AIGC-Editing	Average
		CASIA1.0+	Columbia	Coverage	NIST16	IMD2020	FaceApp	OpenForensics	
pixel-level AUC									
<i>trained methods</i>									
HiFi-Net $\ddagger$ [17]	$\times$	63.4	68.2	71.5	63.7	65.8	61.4	56.7	64.4
PSCC-Net $\ddagger$ [30]	$\times$	76.9	80.6	74.1	69.4	77.2	67.4	<b>68.9</b>	73.5
MVSS-Net $\ddagger$ [11]	$\times$	78.9	79.3	76.5	70.3	76.3	60.9	55.3	71.1
FakeShield $\ddagger$ [54]	$\checkmark$	<b>82.9</b>	83.1	69.6	<u>74.8</u>	<u>80.6</u>	66.2	67.6	75.0
<i>vanilla MLLMs</i>									
GPT-5 [38]	$\checkmark$	69.8	79.6	60.5	71.8	74.6	61.7	56.2	67.7
Gemini 2.5 Pro [15]	$\checkmark$	73.2	78.0	61.3	69.1	78.3	67.5	65.9	70.5
<i>training-free methods</i>									
Noise $\ddagger$ [7, 14, 32]	$\times$	56.1	53.8	59.4	53.9	52.0	52.9	54.1	54.6
Block $\ddagger$ [2, 14]	$\times$	62.5	58.7	58.2	52.8	57.7	49.5	40.9	54.3
Point $\ddagger$ [8, 14, 52]	$\times$	62.3	59.8	74.3	61.5	62.7	57.0	59.0	62.4
Diffusion-LOC [56]	$\times$	58.7	68.2	62.2	55.6	—	—	—	61.2
Foresee(GPT-5)	$\checkmark$	81.5	<b>88.4</b>	<u>80.2</u>	<b>83.5</b>	78.5	<u>68.7</u>	67.2	<u>78.3</u>
Foresee(Gemini 2.5 Pro)	$\checkmark$	<u>82.7</u>	<u>86.7</u>	<b>81.9</b>	72.2	<b>85.2</b>	<b>72.1</b>	<u>68.1</u>	<b>78.4</b>

our method. Among them, CASIA1+ [12], Columbia [34], IMD2020 [36], Coverage [50] and NIST16 [16] are manipulated using traditional image editing tools; FaceApp [1] serves as a deepfake tampering dataset; and OpenForensics [23] comprises samples with AIGC-based editing.

**State-of-the-Art Methods:** To ensure a fair comparison, we select competitive methods that provide either open-source code or pre-trained models. To evaluate the **IFDL performance** of Foresee, we compare it against several SOTA trained methods as well as existing training-free approaches. The trained methods selected in our experiments include HiFi-Net [17], PSCC-Net [30], MVSS-Net [11] and FakeShield [54]. For consistency, all selected models are trained on the MMTD-Set [54] dataset, which encompasses manipulated images from various categories, including editing, deepfake, and AIGC-based editing. The training-free methods evaluated in our experiments include Diffusion-LOC [56], noise-based methods [7, 14, 32], block-based methods [2, 14] and keypoint-based methods [8, 14, 52]. Additionally, to assess the **textual output capability** of Foresee, we compare it with the interpretable forgery detection model FakeShield, as well as proprietary vanilla MLLMs, including GPT-5 [38] and Gemini 2.5 Pro [15].

**Evaluation Metrics:** For forgery detection, we evaluate performance using image-level Area Under the ROC Curve (AUC). For forgery localization, we report pixel-level area under the curve (AUC), F1 scores, and Intersection over Union (IoU). For a fair and comprehensive evaluation of interpretability across all models, we employ GPT-5 as an automatic evaluator to assess the generated textual descriptions along four dimensions: (1) **Accuracy**, measuring how faithfully the description reflects the actual content and context of the manipulated regions; (2) **Level of Detail**, assess-

ing the granularity and specificity of the described forgery artifacts; (3) **Hallucination**, identifying unsupported or irrelevant information not grounded in the image evidence; and (4) **Readability**, examining the fluency, coherence, and overall clarity of the generated text. For detection, a default threshold of 0.5 is applied unless otherwise specified. As SAM2 [39] employs a conservative segmentation strategy within bounding boxes, we lower its probability map threshold to 0.05 to enhance localization accuracy.

**Implementation Details:** Our method is **training-free** and does not require any additional fine-tuning or parameter optimization. For all experiments, we directly employ the proprietary models GPT-5 [38] and Gemini 2.5 Pro [15]. All inference is conducted using the official implementations on a single NVIDIA GeForce RTX 4090 GPU. Default settings are used throughout unless otherwise specified.

## 4.2. Comparison with the State-of-the-Art Methods

To ensure a comprehensive and fair evaluation of model performance in IFDL tasks, our experiments are designed to assess each method at both image-level and pixel-level. To examine the generalization capability of the models, we employ datasets from three distinct categories: editing, deepfake and AIGC-based editing. Furthermore, to evaluate the interpretability of model outputs, we develop a multidimensional assessment framework that scores textual explanations across four criteria.

**Forgery detection evaluation:** To demonstrate the superiority and generalization capability of our method for image forgery detection, we evaluate detection accuracy across three distinct categories of datasets: editing, deepfake and AIGC-based editing. As shown in Table 1, our Foresee achieves a significantly higher image-level AUC than other

Table 3. Localization performance comparison of various IFDL methods and vanilla MLLMs across multiple editing, deepfake, and AIGC-editing datasets, covering both traditional and generative manipulations types. The best and second-best results are highlighted in bold and underline, respectively. Explanation availability is indicated by  $\checkmark/\times$ .  $\dagger$ : Partially self-tested.  $\ddagger$ : Fully self-tested.

Method	Explanation	Editing										DeepFake		AIGC-Editing		Average	
		CASIA1.0+		Columbia		Coverage		NIST16		IMD2020		FaceApp		OpenForensics		IoU	F1
		IoU	F1	IoU	F1												
<i>trained methods</i>																	
HiFi-Net $\ddagger$ [17]	$\times$	13.0	18.0	6.0	11.0	17.2	21.3	9.0	13.0	9.0	14.0	7.0	11.0	2.3	4.1	9.0	13.2
PSCC-Net $\ddagger$ [30]	$\times$	36.0	46.0	64.0	74.0	17.6	22.4	18.0	26.0	22.0	32.0	12.0	18.0	<b>9.4</b>	<b>15.8</b>	25.6	33.5
MVSS-Net $\ddagger$ [11]	$\times$	40.0	48.0	48.0	61.0	21.4	26.8	24.0	29.0	23.0	31.0	9.0	10.0	1.7	3.2	24.1	29.6
FakeShield $\ddagger$ [54]	$\checkmark$	<b>54.0</b>	<b>60.0</b>	<u>67.0</u>	<u>75.0</u>	16.5	19.7	<u>32.0</u>	<u>37.0</u>	<b>50.0</b>	<b>57.0</b>	<u>14.0</u>	<u>22.0</u>	5.9	8.2	34.2	39.8
<i>vanilla MLLMs</i>																	
GPT-5 [38]	$\checkmark$	33.4	37.9	56.1	63.7	10.0	11.3	24.6	26.9	34.1	38.3	1.1	2.1	2.6	3.4	23.1	26.2
Gemini 2.5 Pro [15]	$\checkmark$	35.2	39.3	55.2	61.8	10.6	12.1	21.4	23.9	38.7	43.5	10.3	15.7	9.7	15.0	25.9	30.2
<i>training-free methods</i>																	
Noise $\ddagger$ [7, 14, 32]	$\times$	0.4	0.7	0.2	0.3	12.1	18.1	3.4	4.7	1.9	3.2	0.1	0.1	0.1	0.1	2.6	3.9
Block $\ddagger$ [2, 14]	$\times$	17.0	23.8	15.4	25.2	19.8	24.7	3.8	5.2	3.5	5.8	0.1	0.1	1.5	2.8	8.7	12.5
Point $\ddagger$ [8, 14, 52]	$\times$	13.0	19.2	11.5	15.6	27.6	30.7	3.3	5.8	4.8	6.9	0.1	0.2	2.0	3.5	8.9	11.7
Foresee(GPT-5)	$\checkmark$	43.3	52.1	65.2	<b>77.8</b>	<u>33.4</u>	<b>42.7</b>	<b>39.2</b>	<b>44.4</b>	41.5	45.7	13.8	19.1	4.8	7.2	<u>34.5</u>	<u>41.3</u>
Foresee(Gemini 2.5 Pro)	$\checkmark$	<u>44.1</u>	<u>53.0</u>	<b>67.9</b>	74.6	<b>33.7</b>	<u>42.1</u>	30.3	34.5	<u>45.9</u>	<u>50.9</u>	<b>21.1</b>	<b>28.3</b>	<u>8.5</u>	<u>11.6</u>	<b>35.9</b>	<b>42.1</b>

training-free methods, and attains the best performance on several individual datasets. Notably, in the evaluation of forgery detection, the average image-level AUC of Foresee is only marginally lower than that of the top trained methods, demonstrating the strong generalization capability of our approach. This also indicates that, even without any task-specific training, Foresee exhibits powerful intrinsic forgery detection ability.

**Forgery localization evaluation:** Tables 2 and 3 present the forgery localization results. Our method significantly outperforms other training-free methods and achieves leading pixel-level AUC, IoU, and F1 scores on multiple datasets. Notably, in terms of the average performance across these three metrics, the proposed training-free approach even surpasses the best trained method, highlighting its strong adaptability to diverse data distributions.

Figure 4 illustrates qualitative comparisons of different forgery localization methods. Under the training-free paradigm, Foresee produces cleaner and more complete masks for manipulated regions across diverse data distributions, outperforming other networks in both coverage and precision. In particular, on face-related datasets, other models often focus solely on low-level forgery traces while failing to capture the semantic inconsistencies within facial regions, which limits their ability to provide coherent and accurate localization. These results further verify the generalization ability of Foresee in forgery localization.

**Textual interpretability assessment:** To quantitatively evaluate the quality of the explanatory text generated while localizing tampered regions by different methods, we borrow the powerful reasoning and comprehension capabilities of GPT-5 [38]. Specifically, we randomly sample 200 images from five editing type datasets. For each sample, the potentially manipulated image, the ground-truth image, and the generated textual explanation are jointly provided

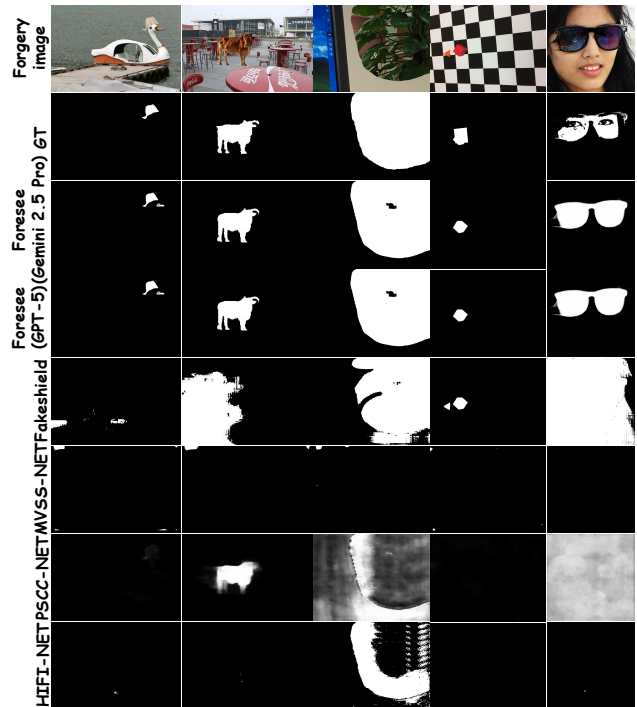


Figure 4. Visual comparison of predicted forgery masks from different methods on representative manipulated images. Ground truth masks and results from several networks are shown for qualitative assessment.

to GPT-5. GPT-5 then scores the textual explanation along four dimensions: accuracy, level of detail, hallucination, and readability, each scored on a five-point scale. This evaluation leverages the multimodal reasoning capabilities of MLLMs to provide a more holistic and human-aligned assessment compared to traditional automatic metrics such as cosine semantic similarity. As shown in Table 4, our method achieves the highest scores across all four dimensions. These results indicate that the textual explanations

Table 4. Comparative results of vanilla MLLMs and explainable models in the image forgery detection and localization domain across different editing datasets. The best and second-best results are highlighted in bold and underline, respectively.

Method	Accuracy	Details	Hallucination	Readability	Average
<i>vanilla MLLMs</i>					
GPT-5 [38]	1.26	4.10	2.22	4.94	3.13
Gemini 2.5 Pro [15]	0.89	4.25	1.40	<b>5.00</b>	2.89
<i>explainable models for image forgery detection domain</i>					
FakeShield [54]	2.41	4.44	3.07	<u>4.95</u>	3.72
Foresee(GPT-5)	<b>3.18</b>	4.18	<b>3.56</b>	4.92	<u>3.91</u>
Foresee(Gemini 2.5 Pro)	<u>3.07</u>	<b>4.60</b>	<b>3.26</b>	<b>5.00</b>	<b>3.98</b>

generated by our model not only describe the manipulated regions with high precision, but also provide rich and detailed context. Moreover, our outputs effectively suppress hallucinations, ensuring reliability, and exhibit superior fluency and readability.

**Robustness study:** To assess the robustness of our method against common transmission degradations, we evaluate Foresee on the CASIA1+ [12] and Columbia [34] datasets under four degradation types: JPEG compression (quality factors of 70 and 80) and Gaussian noise (variances of 5 and 10). Performance across these degradation settings is summarized in Table 5. As shown, Foresee exhibits minimal performance degradation under Gaussian noise and JPEG compression, demonstrating strong robustness in forgery localization even when image details are partially lost.

Table 5. Localization performance on CASIA1.0+ and Columbia datasets under different degradation conditions.

Method	CASIA1.0+			Columbia		
	AUC	IoU	F1	AUC	IoU	F1
JPEG 70	79.5	42.8	48.9	86.9	64.7	73.7
JPEG 80	79.7	42.9	49.1	87.3	64.9	73.9
Gaussian 5	78.9	42.0	48.5	85.9	64.0	72.7
Gaussian 10	77.1	41.2	47.7	84.4	61.5	70.5
Foresee (GPT-5)	81.5	43.3	52.1	88.4	65.2	77.8

### 4.3. Ablation Study

This section analyzes the effectiveness of the type-prior strategy and the Flexible Feature Detector (FFD) module within the Foresee pipeline. We also conduct an ablation study on the choice of vanilla MLLMs employed in our framework.

Table 6. Localization performance of Foresee with and without the type-prior strategy on multiple diverse datasets.

Method	CASIA1.0+		Coverage		NIST16	
	IoU	F1	IoU	F1	IoU	F1
Foresee(GPT-5) w/o type-prior	34.5	39.6	12.0	13.6	23.2	25.3
Foresee(GPT-5)	43.3	52.1	33.4	42.7	39.2	44.4

**Ablation on type-prior strategy:** As shown in Table 6, incorporating type prediction and corresponding prompt selection notably enhances the localization performance of

Foresee across all datasets. This demonstrates that adapting the prompting process with prior knowledge of manipulation type is crucial for achieving accurate and consistent forgery localization.

Table 7. Localization performance of Foresee with and without FFD module on copy-move datasets.

Method	CASIA1.0+(CM)			Coverage		
	AUC	IoU	F1	AUC	IoU	F1
Foresee(GPT-5) w/o FFD	60.2	11.6	16.0	67.7	23.2	28.9
Foresee(GPT-5)	76.8	24.2	31.4	80.2	33.4	42.7

**Ablation on Flexible Feature Detector (FFD):** We perform ablation experiments on Coverage [50] and the *copy-move* subsets of CASIA1+ [12] datasets to evaluate the effectiveness of our FFD module. As shown in Table 7, integrating FFD substantially enhances the localization performance of Foresee on *copy-move* datasets. These results suggest that the FFD module effectively compensates for the limitations of vanilla MLLMs in capturing repetitive textures and local structural similarities, thereby enhancing their ability to detect *copy-move* forgeries.

Table 8. Localization performance of Foresee with different MLLMs on CASIA1.0+ and Columbia datasets

Method	CASIA1.0+			Columbia		
	AUC	IoU	F1	AUC	IoU	F1
Foresee(Qwen3-VL)	78.0	38.7	46.5	79.8	60.9	68.9
Foresee(Claude Sonnet 4)	77.2	36.2	44.6	78.3	46.2	52.8
Foresee(GPT-5)	81.5	43.3	52.1	88.4	65.2	77.8
Foresee(Gemini 2.5 Pro)	82.7	44.1	53.0	86.7	67.9	74.6

**Choices of vanilla MLLMs:** Ablation results in Table 8 show that the choice of vanilla MLLMs has a notable impact on localization performance. Models powered by GPT-5 [38] and Gemini 2.5 Pro [15] consistently achieve superior results on CASIA1+ [12] and Columbia [34] datasets compared with those based on Qwen3-VL [9] and Claude Sonnet 4 [3], highlighting the importance of advanced multimodal reasoning capabilities for forgery localization.

## 5. Conclusion

In this work, we introduce Foresee, a novel training-free pipeline for image forgery detection and localization (IFDL) that leverages the generalization potential of vanilla multimodal large language models (MLLMs). Foresee achieves strong generalization across diverse manipulation types and produces superior textual interpretations under multiple evaluation criteria. By employing a type-prior-driven strategy and utilizing a Flexible Feature Detector (FFD) module to specifically handle copy-move manipulations, Foresee demonstrates the generalization potential of vanilla MLLMs for forensics domain. Extensive experiments demonstrate that our work represents a significant

advancement toward fully training-free and generalizable IFDL solutions, establishing Foresee as a solid foundation for future research in interpretable and multimodal image forensics. Foresee provides new insights into the intrinsic generalization capabilities of MLLMs and highlights their potential for broader visual understanding tasks.

## References

- [1] FaceApp: Mobile photo editor application. <https://www.faceapp.com/>, 2017. 6
- [2] Irene Amerini, Lamberto Ballan, Roberto Caldelli, Alberto Del Bimbo, and Giuseppe Serra. A sift-based forensic method for copy-move attack detection and transformation recovery. *IEEE transactions on information forensics and security*, 6(3):1099–1110, 2011. 3, 5, 6, 7
- [3] Anthropic. Claude sonnet 4. <https://www.anthropic.com>, 2024. Accessed: Nov. 2024. 2, 3, 8
- [4] Jinze Bai, Shuai Bai, Yunfei Chu, Zeyu Cui, Kai Dang, Xiaodong Deng, Yang Fan, Wenbin Ge, Yu Han, Fei Huang, et al. Qwen technical report. *arXiv preprint arXiv:2309.16609*, 2023. 2
- [5] Lucy Chai, David Bau, Ser-Nam Lim, and Phillip Isola. What makes fake images detectable? understanding properties that generalize. In *European conference on computer vision*, pages 103–120. Springer, 2020. 4
- [6] Jun Chen, Deyao Zhu, Xiaoqian Shen, Xiang Li, Zechun Liu, Pengchuan Zhang, Raghuraman Krishnamoorthi, Vikas Chandra, Yunyang Xiong, and Mohamed Elhoseiny. Minigt-v2: large language model as a unified interface for vision-language multi-task learning. *arXiv preprint arXiv:2310.09478*, 2023. 3
- [7] Mo Chen, Jessica Fridrich, Miroslav Goljan, and Jan Lukás. Determining image origin and integrity using sensor noise. *IEEE Transactions on information forensics and security*, 3(1):74–90, 2008. 4, 5, 6, 7
- [8] Vincent Christlein, Christian Riess, Johannes Jordan, Corinna Riess, and Elli Angelopoulou. An evaluation of popular copy-move forgery detection approaches. *IEEE Transactions on information forensics and security*, 7(6):1841–1854, 2012. 3, 4, 5, 6, 7
- [9] Alibaba Cloud. Qwen3-vl-235b. <https://qwenlm.github.io/>, 2024. Accessed: Nov. 2024. 2, 8
- [10] Davide Cozzolino, Giovanni Poggi, and Luisa Verdoliva. Splicebuster: A new blind image splicing detector. In *2015 IEEE International Workshop on Information Forensics and Security (WIFS)*, pages 1–6. IEEE, 2015. 4
- [11] Chengbo Dong, Xinru Chen, Ruohan Hu, Juan Cao, and Xirong Li. Mvss-net: Multi-view multi-scale supervised networks for image manipulation detection. *IEEE Transactions on Pattern Analysis and Machine Intelligence*, 45(3):3539–3553, 2022. 2, 3, 5, 6, 7
- [12] Jing Dong, Wei Wang, and Tieniu Tan. Casia image tampering detection evaluation database. In *2013 IEEE China summit and international conference on signal and information processing*, pages 422–426. IEEE, 2013. 6, 8
- [13] Hany Farid. Image forgery detection. *IEEE Signal processing magazine*, 26(2):16–25, 2009. 4
- [14] Jessica Fridrich, David Soukal, Jan Lukas, et al. Detection of copy-move forgery in digital images. In *Proceedings of digital forensic research workshop*, pages 652–63. Cleveland, OH, 2003. 3, 4, 5, 6, 7
- [15] Google. Gemini api models: Gemini 2.5. <https://gemini.google.com/app?hl=zh-cn>, 2025. Accessed: 2025-10-22. 2, 3, 5, 6, 7, 8
- [16] Haiying Guan, Mark Kozak, Eric Robertson, Yooyoung Lee, Amy N Yates, Andrew Delgado, Daniel Zhou, Timothee Kheyrkhan, Jeff Smith, and Jonathan Fiscus. Mfc datasets: Large-scale benchmark datasets for media forensic challenge evaluation. In *2019 IEEE Winter Applications of Computer Vision Workshops (WACVW)*, pages 63–72. IEEE, 2019. 6
- [17] Xiao Guo, Xiaohong Liu, Zhiyuan Ren, Steven Grosz, Iacopo Masi, and Xiaoming Liu. Hierarchical fine-grained image forgery detection and localization. In *Proceedings of the IEEE/CVF Conference on Computer Vision and Pattern Recognition (CVPR)*, 2023. 2, 3, 5, 6, 7
- [18] Xuefeng Hu, Zhihan Zhang, Zhenye Jiang, Syomantak Chaudhuri, Zhenheng Yang, and Ram Nevatia. Span: Spatial pyramid attention network for image manipulation localization. In *European conference on computer vision*, pages 312–328. Springer, 2020. 3
- [19] Aaron Hurst, Adam Lerer, Adam P Goucher, Adam Perelman, Aditya Ramesh, Aidan Clark, AJ Ostrow, Akila Welihinda, Alan Hayes, Alec Radford, et al. Gpt-4o system card. *arXiv preprint arXiv:2410.21276*, 2024. 2
- [20] Ashrafal Islam, Chengjiang Long, Arslan Basharat, and Anthony Hoogs. Doa-gan: Dual-order attentive generative adversarial network for image copy-move forgery detection and localization. In *Proceedings of the IEEE/CVF conference on computer vision and pattern recognition*, pages 4676–4685, 2020. 3
- [21] Takeshi Kojima, Shixiang Shane Gu, Machel Reid, Yutaka Matsuo, and Yusuke Iwasawa. Large language models are zero-shot reasoners. *Advances in neural information processing systems*, 35:22199–22213, 2022. 3
- [22] Myung-Joon Kwon, In-Jae Yu, Seung-Hun Nam, and Heung-Kyu Lee. Cat-net: Compression artifact tracing network for detection and localization of image splicing. In *Proceedings of the IEEE/CVF winter conference on applications of computer vision*, pages 375–384, 2021. 2, 3
- [23] Trung-Nghia Le, Huy H Nguyen, Junichi Yamagishi, and Isao Echizen. Openforensics: Large-scale challenging dataset for multi-face forgery detection and segmentation in-the-wild. In *Proceedings of the IEEE/CVF international conference on computer vision*, pages 10117–10127, 2021. 6
- [24] Haodong Li and Jiwu Huang. Localization of deep inpainting using high-pass fully convolutional network. In *proceedings of the IEEE/CVF international conference on computer vision*, pages 8301–8310, 2019. 3
- [25] Haodong Li, Weiqi Luo, Xiaoqing Qiu, and Jiwu Huang. Image forgery localization via integrating tampering possibility maps. *IEEE Transactions on Information Forensics and Security*, 12(5):1240–1252, 2017. 4
- [26] Junnan Li, Dongxu Li, Silvio Savarese, and Steven Hoi. Blip-2: Bootstrapping language-image pre-training with

- frozen image encoders and large language models. In *International conference on machine learning*, pages 19730–19742. PMLR, 2023. 3
- [27] Yuanman Li and Jiantao Zhou. Fast and effective image copy-move forgery detection via hierarchical feature point matching. *IEEE Transactions on Information Forensics and Security*, 14(5):1307–1322, 2018. 3
- [28] Haotian Liu, Chunyuan Li, Qingyang Wu, and Yong Jae Lee. Visual instruction tuning. *Advances in neural information processing systems*, 36:34892–34916, 2023. 2, 3
- [29] Shilong Liu, Zhaoyang Zeng, Tianhe Ren, Feng Li, Hao Zhang, Jie Yang, Qing Jiang, Chunyuan Li, Jianwei Yang, Hang Su, et al. Grounding dino: Marrying dino with grounded pre-training for open-set object detection. In *European conference on computer vision*, pages 38–55. Springer, 2024. 4
- [30] Xiaohong Liu, Yaojie Liu, Jun Chen, and Xiaoming Liu. Psc-c-net: Progressive spatio-channel correlation network for image manipulation detection and localization. *IEEE Transactions on Circuits and Systems for Video Technology*, 32(11):7505–7517, 2022. 2, 3, 5, 6, 7
- [31] Andreas Lugmayr, Martin Danelljan, Andres Romero, Fisher Yu, Radu Timofte, and Luc Van Gool. Repaint: Inpainting using denoising diffusion probabilistic models. In *Proceedings of the IEEE/CVF conference on computer vision and pattern recognition*, pages 11461–11471, 2022. 4
- [32] Jan Lukáš, Jessica Fridrich, and Miroslav Goljan. Detecting digital image forgeries using sensor pattern noise. In *Security, steganography, and watermarking of multimedia contents VIII*, pages 362–372. SPIE, 2006. 5, 6, 7
- [33] Xiaochen Ma, Bo Du, Zhuohang Jiang, Ahmed Y Al Hammedi, and Jizhe Zhou. Iml-vit: Benchmarking image manipulation localization by vision transformer. *arXiv preprint arXiv:2307.14863*, 2023. 2, 3, 4
- [34] Tian-Tsong Ng, Jessie Hsu, and Shih-Fu Chang. Columbia image splicing detection evaluation dataset. *DVMM lab. Columbia Univ CalPhotos Digit Libr*, 2009. 6, 8
- [35] Yuval Nirkin, Lior Wolf, Yosi Keller, and Tal Hassner. Deepfake detection based on discrepancies between faces and their context. *IEEE transactions on pattern analysis and machine intelligence*, 44(10):6111–6121, 2021. 4
- [36] Adam Novozamsky, Babak Mahdian, and Stanislav Saic. Imd2020: A large-scale annotated dataset tailored for detecting manipulated images. In *Proceedings of the IEEE/CVF Winter Conference on Applications of Computer Vision Workshops*, pages 71–80, 2020. 6
- [37] OpenAI. Openai sora system card, 2024. Available at: <https://openai.com/research/sora-system-card> (Accessed: 2025-10-22). 2
- [38] OpenAI. Introducing gpt-5. <https://openai.com/blog/introducing-gpt-5>, 2025. Accessed: 2025-10-22. 2, 3, 5, 6, 7, 8
- [39] Nikhila Ravi, Valentin Gabeur, Yuan-Ting Hu, Ronghang Hu, Chaitanya Ryali, Tengyu Ma, Haitham Khedr, Roman Rädle, Chloe Rolland, Laura Gustafson, et al. Sam 2: Segment anything in images and videos. *arXiv preprint arXiv:2408.00714*, 2024. 4, 6
- [40] Robin Rombach, Andreas Blattmann, Dominik Lorenz, Patrick Esser, and Björn Ommer. High-resolution image synthesis with latent diffusion models. In *Proceedings of the IEEE/CVF conference on computer vision and pattern recognition*, pages 10684–10695, 2022. 2
- [41] Chitwan Saharia, William Chan, Saurabh Saxena, Lala Li, Jay Whang, Emily L Denton, Kamyar Ghasemipour, Raphael Gontijo Lopes, Burcu Karagol Ayan, Tim Salimans, et al. Photorealistic text-to-image diffusion models with deep language understanding. *Advances in neural information processing systems*, 35:36479–36494, 2022. 2
- [42] Ronald Salloum, Yuzhuo Ren, and C-C Jay Kuo. Image splicing localization using a multi-task fully convolutional network (mfcn). *Journal of Visual Communication and Image Representation*, 51:201–209, 2018. 3
- [43] Gemini Team, Rohan Anil, Sebastian Borgeaud, Jean-Baptiste Alayrac, Jiahui Yu, Radu Soricut, Johan Schalkwyk, Andrew M Dai, Anja Hauth, Katie Millican, et al. Gemini: a family of highly capable multimodal models. *arXiv preprint arXiv:2312.11805*, 2023. 2
- [44] Ruben Tolosana, Ruben Vera-Rodriguez, Julian Fierrez, Aythami Morales, and Javier Ortega-Garcia. Deepfakes and beyond: A survey of face manipulation and fake detection. *Information Fusion*, 64:131–148, 2020. 4
- [45] Qinyue Tong, Ziqian Lu, Jun Liu, Yangming Zheng, and Zheming Lu. Medisee: Reasoning-based pixel-level perception in medical images. *arXiv preprint arXiv:2504.11008*, 2025. 2, 3
- [46] Luisa Verdoliva. Media forensics and deepfakes: an overview. *IEEE journal of selected topics in signal processing*, 14(5):910–932, 2020. 4
- [47] Mengxi Wang, Shaozhang Niu, and Jiwei Zhang. Forgdiffuser: General image forgery localization with diffusion models. 3
- [48] Peng Wang, Shuai Bai, Sinan Tan, Shijie Wang, Zhihao Fan, Jinze Bai, Keqin Chen, Xuejing Liu, Jialin Wang, Wenbin Ge, et al. Qwen2-vl: Enhancing vision-language model’s perception of the world at any resolution. *arXiv preprint arXiv:2409.12191*, 2024. 2
- [49] Jason Wei, Xuezhi Wang, Dale Schuurmans, Maarten Bosma, Fei Xia, Ed Chi, Quoc V Le, Denny Zhou, et al. Chain-of-thought prompting elicits reasoning in large language models. *Advances in neural information processing systems*, 35:24824–24837, 2022. 3
- [50] Bihan Wen, Ye Zhu, Ramanathan Subramanian, Tian-Tsong Ng, Xuanjing Shen, and Stefan Winkler. Coverage—a novel database for copy-move forgery detection. In *2016 IEEE international conference on image processing (ICIP)*, pages 161–165. IEEE, 2016. 6, 8
- [51] Haiwei Wu, Jiantao Zhou, Jinyu Tian, and Jun Liu. Robust image forgery detection over online social network shared images. In *Proceedings of the IEEE/CVF Conference on Computer Vision and Pattern Recognition*, pages 13440–13449, 2022. 3
- [52] Yue Wu, Wael Abd-Almageed, and Prem Natarajan. Buster-net: Detecting copy-move image forgery with source/target localization. In *Proceedings of the European conference on computer vision (ECCV)*, pages 168–184, 2018. 3, 5, 6, 7

- [53] Yue Wu, Wael AbdAlmageed, and Premkumar Natarajan. Mantra-net: Manipulation tracing network for detection and localization of image forgeries with anomalous features. In *Proceedings of the IEEE/CVF conference on computer vision and pattern recognition*, pages 9543–9552, 2019. [3](#)
- [54] Zhipei Xu, Xuanyu Zhang, Runyi Li, Zecheng Tang, Qing Huang, and Jian Zhang. Fakeshield: Explainable image forgery detection and localization via multi-modal large language models. *arXiv preprint arXiv:2410.02761*, 2024. [2](#), [3](#), [5](#), [6](#), [7](#), [8](#)
- [55] Zeqin Yu, Jiangqun Ni, Yuzhen Lin, Haoyi Deng, and Bin Li. Diffforensics: Leveraging diffusion prior to image forgery detection and localization. In *Proceedings of the IEEE/CVF Conference on Computer Vision and Pattern Recognition*, pages 12765–12774, 2024. [2](#), [3](#)
- [56] Zhenfei Zhang, Ming-Ching Chang, and Xin Li. Training-free image manipulation localization using diffusion models. In *Proceedings of the AAAI Conference on Artificial Intelligence*, pages 10376–10384, 2025. [2](#), [3](#), [6](#)
- [57] Deyao Zhu, Jun Chen, Xiaoqian Shen, Xiang Li, and Mohamed Elhoseiny. Minigpt-4: Enhancing vision-language understanding with advanced large language models. *arXiv preprint arXiv:2304.10592*, 2023. [2](#), [3](#)
- [58] Xinshan Zhu, Yongjun Qian, Xianfeng Zhao, Biao Sun, and Ya Sun. A deep learning approach to patch-based image inpainting forensics. *Signal Processing: Image Communication*, 67:90–99, 2018. [3](#)